MSc Thesis Proposal
(working draft)
October 28, 2020

Kurtis Anstey
V00939802
Department of Physics and Astronomy
University of Victoria

Dr. Jody Klymak
Dr. Steven Mihaly
Dr. Richard Thomson

Contents

1 Introduction

This research seeks to characterise the internal wave field at Barkley Canyon, off the coast of Vancouver Island, to provide information regarding regional mixing processes and what drives them. This is important for understanding transport of nutrients, heat, O_2, and CO_2, which affect both climate and biological productivity. This research makes use of time-series data of unprecedented temporal and spatial characteristics to build on a body of research involving interactions of internal waves with canyon topography, and related processes in the Vancouver Island Continental Shelf region.

1.1 Internal waves and tides

Internal waves are slow-moving, low-frequency gravity waves that exist due to density gradients below the oceans' surface (Garrett & Munk, 1979). They can have wavelengths up to kilometres long, and oscillate in a range between the Coriolis and Brunt–Väisälä (buoyancy) frequencies (Garrett & Munk, 1979). They are often caused by the wind, or tides and currents moving over irregular seafloor topography, such as sea mounts, continental shelves, and canyons; this generates waves that travel outward from their origin through the stratified ocean (Hendershott & Garrett, 2018). Internal waves propagate through the depths, and if arriving at a boundary, topography can cause scattering, reflection, or breaking events such as internal bores (Martini et al., 2013).

The interior of the ocean is never calm, and internal waves have been observed since the onset of physical oceanography; as early as the early 20th century, classical oceanographers reported consistent small-scale noise in their hydrocast readings (Garrett & Munk, 1979). Even then, internal waves were no mystery; theory surrounding their presence was developed as early as the mid-19th century, with notable scientists such as Stokes and Rayleigh discussing fluid density interfaces and continuous stratification (Garrett & Munk, 1979). Ekman made note of them in his turn-of-the-century publications, and Garrett and Munk (1979) later developed their classical Garrett-Munk (GM) spectrum to define the characteristic frequency and wavenumber continuum associated with internal waves. As the 21st century approached, the temporal and spatial resolution of instruments improved, and through the use of research platforms such as FLIP, and sensitive instrumentation such as Acoustic Doppler Current Profilers (ADCP), scientists continued to uncover the broad importance of internal waves (Garrett & Munk, 1979). Currently, the field is burgeoning with research opportunity, as there is still debate on issues such as internal wave generation and dissipation (Terker et al., 2014; Kunze, 2017), scattering and reflection on continental slopes (Nash et al., 2004; Kunze et al., 2012;

Gemmrich & Klymak, 2015), and forcing response due to seasonal weather variability (Alford et al., 2012; Thomson & Krassovski, 2015), all of which are associated with internal waves interacting with irregular topography.

As internal waves and tides approach coastal topography, their energy forces important mixing. The topography focuses their energy, which cascades from low- to high-frequency processes, and eventually dissipates as heat (Garrett & Munk, 1979). This dissipation creates an energetic local environment, and is evident as mixing processes on the fine- (1 m to 100 m vertical) and micro-scales (less than 1 m vertical) (Garrett & Munk, 1979; Kunze et al., 2012). These processes play a significant role in the regional transport of energy and momentum, and the mixing of heat, pollutants, and biological constituents (Kunze et al., 2012). Furthermore, internal waves are crucial for setting ocean stratification, layers that drive important large-scale systems such as overturning circulation (Garrett & Munk, 1979). As such, a better understanding of internal waves interacting with topography is also important for predicting changes in the coupled ocean-atmosphere climate system (Garrett & Munk, 1979).

As irregular topography appears to be a hot spot for internal wave generation and dissipation, notable studies have been ongoing at the Hawaiian ridge (Alford et al., 2007), in the South China Sea (Klymak et al., 2011), and in the canyons of the eastern Pacific (Allen et al., 2001; Carter & Gregg, 2002; Kunze et al., 2012; Terker et al., 2014). Research has found that canyons contribute to internal wave generation due to forced inflow by tides and regional currents (Carter & Gregg, 2002). Canyon topography not only generates, but dissipates internal waves, by focusing incident energy into cascading low- to high-frequency processes, leading to breaking internal bores and upwelling events (Allen et al., 2001). Monterey Canyon in California has provided important information on critical slopes scattering and reflecting incoming internal waves (Kunze et al., 2012), the presence of internal-bores and near-bottom turbulent layers that drive mixing (Carter & Gregg, 2002), and correlation between specific topographical features with increased dissipation rates and internal tide generation (Terker et al., 2014).

The success of topographic internal wave studies has led to research further along the northeast Pacific coast, with observations off of Oregon (Martini et al., 2013) and Washington (Allen et al., 2001), in addition to Monterey Canyon. Canada is no exception, with research focused on the Vancouver Island Continental Shelf. This region has currents associated with the northeast Pacific seasonal current cycles (Thomson & Krassovski, 2015), potential non-linear wave-wave interaction between near-inertial internal waves and semidiurnal

internal tides (Mihaly et al., 1998), and seasonal forcing by surface winds for near-inertial internal waves (Alford et al., 2012). Interesting observations of vorticity and upwelling were found in Barkley Canyon due to the seasonally variable currents, causing considerable canyon influence on local water properties and the regional transport of biological constituents (Allen et al., 2001). As such, further research at Barkley Canyon is necessary for improving understanding of regional processes that are related to internal waves, and their driving factors.

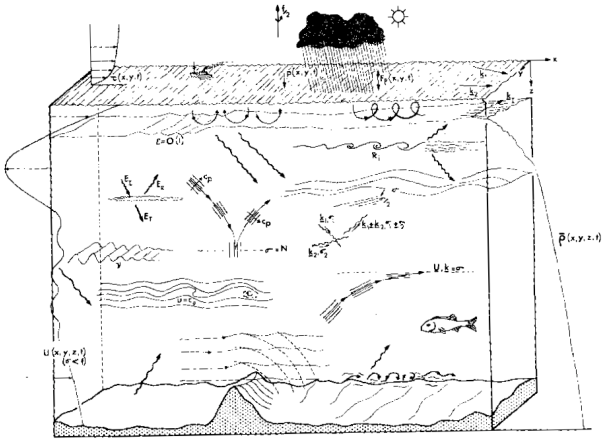

Figure 1: General depiction of internal wave processes in the ocean, as envisioned by Garrett and Munk (1979).

1.2 Barkley Canyon

The data for this research is from Barkley Canyon, and is extraordinary for both temporal and spatial consideration. Located at 48.33°N and 126.03°W, Barkley Canyon is about 100 km southwest of Vancouver Island, with a rim and axis at depths of approximately -400 and -900 m, respectively (Barkley Canyon, 2013). At various locations along the topography of the canyon, ADCP and other vertical profiling instruments are operated by Ocean Networks Canada (ONC) to provide velocity data, along with climatology and other important regional information (ONC, 2013). The available time series for local ADCP is over ten years, allowing for analysis of multi-year and decade variability that is previously unexplored. Furthermore, the critical placement of multiple ADCP instruments provides an opportunity for a comprehensive spatial analysis of internal wave effects as they propagate through and above the canyon, impossible with a single moored instrument or short-term dropped observations.

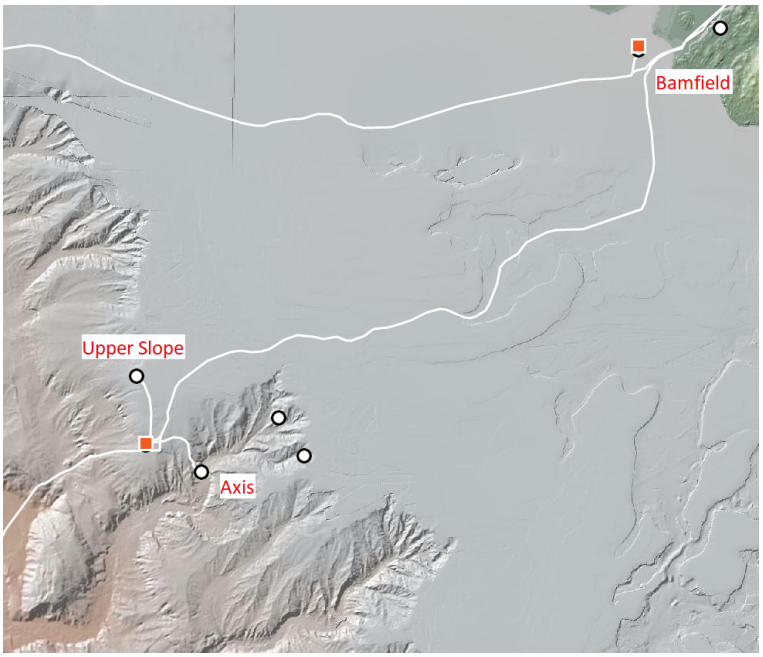

Figure 2: General map of the Barkley Canyon region, about 100 km southwest from Bamfield, on Vancouver Island. Circles represent local ONC instrument moorings, with the relevant Axis and Upper Slope ADCP instruments indicated. Adapted from the ONC Oceans 2.0 research portal.

1.3 Data acquisition

Acoustic Doppler Current Profiler (ADCP) instruments send out multiple acoustic beams that measure and triangulate Doppler shifts in the vertical water column, providing directional velocity data through time, and at spatial resolutions dependent on the operating frequency of the instrument. In the Barkley Canyon region, ONC's Oceans 2.0 data portal offers publicly available data covering over 10 years, from 2009 to present, for multiple ADCP instruments, at a sampling rate of 2-seconds. The ADCP and their data are both configured and maintained as ready-to-use by ONC. Relevant ADCP were chosen as the Axis (75 kHz and 55 kHz), Upper Slope (75 kHz), and Mid-East* (150 kHz) nodes. Complete datasets were initially downloaded in NetCDF format at a resolution of 1-hour, to check data quality. Some issues were noted with the Mid-East 150 kHz beams, and sent to ONC for revision, and are pending their review. Axis 75 kHz and Upper Slope 75 kHz both appear to offer reliable data, albeit with some significant data gaps in time, and noise at the extremes of the acoustic beam depth range. These two instruments are expected to be the primary data sources for this research. Overlapping quality coverage is primarily during 2013, 2014, 2017, and 2018, though specific comparisons will be possible for other years and seasons. The potential use of

the Axis 55 kHz (pending conversion) and Mid-East 150 kHz ADCP (pending ONC revision) could add to this coverage.

Axis - 75 kHz ADCP - Depth 968 metres (near canyon bottom)
Upper Slope - 75 kHz ADCP - Depth 378 metres (canyon adjacent plateau)
*Mid-East (150 kHz) $\sim$ 900 m

After the initial quality check, complete datasets for Axis 75 kHz and Upper Slope 75 kHz ADCP were downloaded in NetCDF format at a resolution of 15-minutes, determined as adequate averaging of the data for resolving frequencies and wave events on the spatial and temporal time-scales necessary for the science objectives of this research.

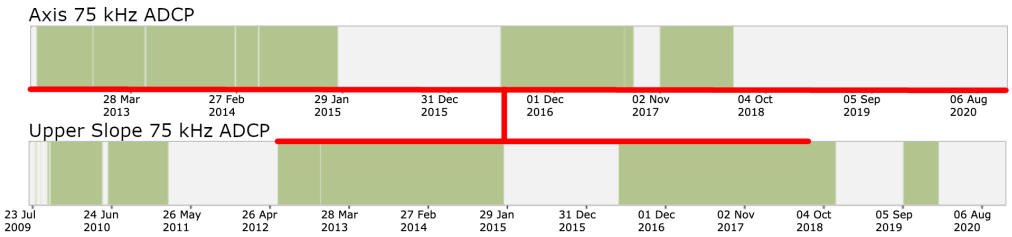

Figure 3: ONC Oceans 2.0 supplied plots of data coverage for the Axis 75 kHz, and Upper Slope 75 kHz ADCPs, respectively.

2 Project goals

2.1 Thesis

This research seeks to characterise the internal wave field at Barkley Canyon, off of Vancouver Island, to provide information regarding local and regional mixing processes and, ideally, what drives them. This will include an analysis of variability in regional mean currents, tides, and surface winds, to identify forcing. Forcing will be correlated to observable internal wave events within the canyon, and association expanded to dissipative processes that may affect regional systems. This will be accomplished by:

- Identifying trends in low-pass filtered and rotated velocity data will identify regional mean currents, such as the VICS segment of the Northeast Pacific Coastal Current (NPCC), as potential drivers for internal wave generation or dissipation. The noted mean currents likely have a temporal dependence, so trends will be compared between seasons, annually, and multi-annually, and with regional weather data for further evidence of forcing. Spatially, the data will be evaluated for direction and depth, to evaluate topographic influence on internal waves. A similar analysis of super-inertial velocity data will identify prominent diurnal and semidiurnal tidal constituents. As with the low-pass data, direction, depth, and temporal variability in these flows will be evaluated to constrain seasonal and tidal forcing, and may suggest the presence of topography dependent high-frequency dissipative processes.
- To confirm and refine velocity observations, spectral analysis (power spectra, rotary spectra, and spectrograms) in both one- and two-dimension(s) will provide estimates of the relative power, rotation, and temporal and spatial dependencies of notable frequency constituents in the tidal, near-inertial, and super-inertial bands. Temporally, this can be compared to the observed seasonal forcing by the wind and mean currents, and regular tidal cycles, to reinforce their correlation. Furthermore, a spatial comparison through depth may indicate topographic dependencies for sources of forcing or potential high-frequency dissipative processes.
- Finally, the shape and amplitude of the continuum will be characterised and compared to observed seasonality to check for its presence in the broadband. As the state of the continuum is thought to be related to the rate of energy dissipation in the system, an attempt will be made to correlate seasonal variability in energy levels to local dissipation rates (Carter & Gregg, 2002). Furthermore, the characterised spectral continuum can be compared with the classical open ocean GM spectrum,

locally calibrated, for insight into the state of the canyon's focused internal wave field in relation to accepted physical theory for internal waves in open water.

2.2 Optional goals

There are many other forms of internal wave analysis that could be included to expand on the proposed goals, but that may be beyond the limited scope of this research as an MSc project. Optional goals could include:

- An analysis of critical slope angles for the VICS near the Barkley Canyon mouth, and the efficiency of associated internal wave reflection and/or scattering in this region.
- A search for evidence of non-linearity in the time series, which could suggest non-linear wave-wave interaction and energy loss between wind generated downward propagating internal waves and canyon generated upward propagating internal tides (Mihaly et al., 1998).
- A report to ONC with useful data quality assessment, instrument calibration feedback, and data analysis processes, to assist in the successful outcomes of continued research along the VICS.

2.3 Prospective time line

- December 2020: Complete final required course.
- January 2021: Complete preliminary analysis. Begin writing thesis.
- March/April 2021: Finish thesis. Schedule thesis defence.
- May/June 2021: Defend thesis.

3 Preliminary methods and analysis

All plots and analyses are to be considered works-in-progress, and as samples to highlight the potential of this research.

Preliminary analysis has been carried out using ONC Oceans 2.0 for data acquisition, Python and Jupyter Notebook for data processing, LaTeX and BibDesk for document creation, and GitHub (kurtisanstey/project) for file hosting. Other relevant packages and resources are mentioned when necessary.

Specific details of data analysis methods can be found in the relevant Jupyter Notebook project files, hosted on the listed GitHub repository, and a comprehensive list of notable results can be found in a separate Analysis document, available upon request. Each form of analysis is available for seasonal, annual, and multi-year comparison, per and between instruments.

3.1 Velocities

Velocity data were truncated and NaN values interpolated to improve temporal quality, and to remove noise at the extreme depth limits of each instrument. Data were filtered to highlight differences in the mean currents and tides, by applying a 40-hour digital low-pass Butterworth filter and examining the low-pass versus the super-inertial data. Data were rotated using Euler's formula

$$\underline{u}_{rot} = \underline{u}e^{-i\theta}$$

to better match the cross-slope angle of approximately +30°, to help identify relationships between the predominant VICS currents and local canyon topography; u is referred to as 'cross-slope', and v is 'along-slope'.

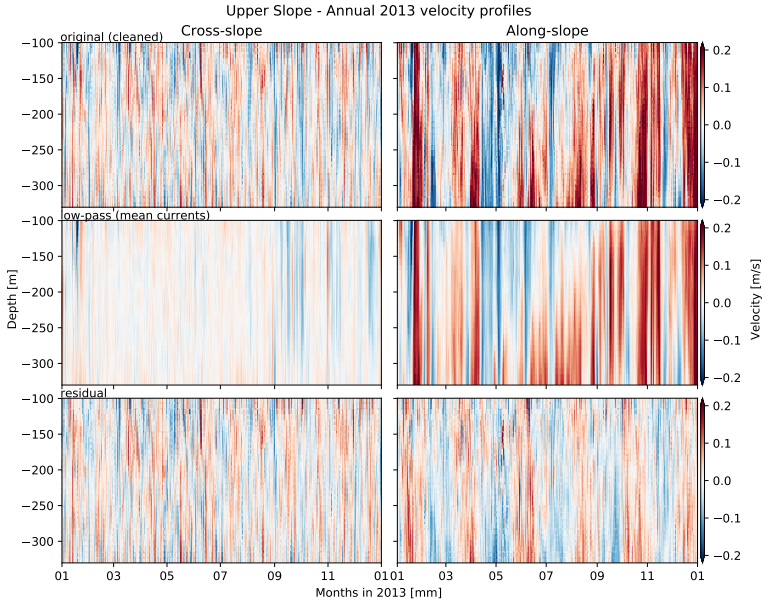

(a) Upper Slope - 2013

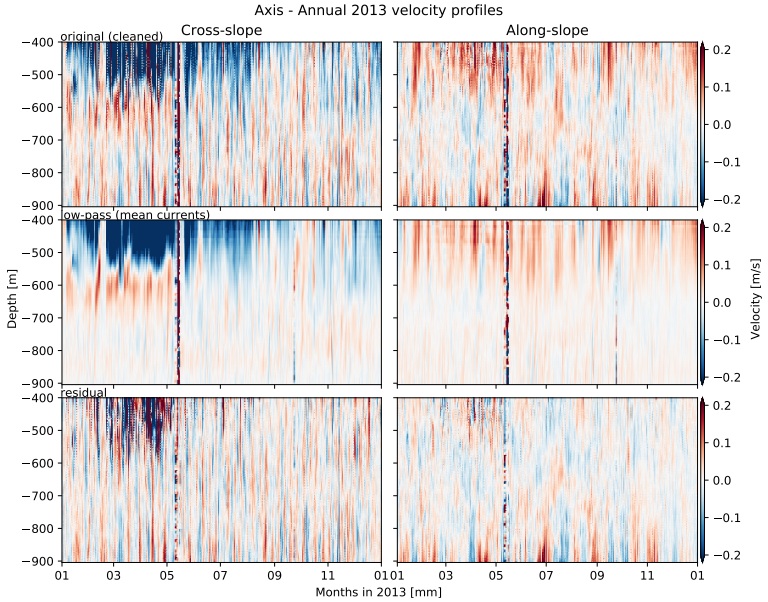

(b) Axis - 2013

Figure 4: Sample velocity data for Upper Slope 75 kHz and Axis 75 kHz ADCP in 2013. Velocities are displayed horizontally in cross- (left) and along-slope (right) directions, and vertically as unfiltered (top), low-pass (middle), and residual (bottom) data. The 15-minute resolution velocity data has been cleaned to account for NaN gaps, extreme depth interference, and rotated to match the continental slope angle of approximately 30°.

Notable trends in velocity data include a seasonal switch in mean currents from NW to SE during the spring, at upper depths (Upper Slope 75 kHz ADCP), potentially corresponding to variability in the NPCC. Also for Upper Slope, there is seasonal variability in apparent two-week pulses that could correspond with the spring neap cycle, as it interacts with the NPCC. Velocities are dominant in the along-slope direction for Upper Slope 75 kHz ADCP, and cross-slope near the canyon floor (Axis 75 kHz ADCP). For Axis, there is less seasonality, and fairly consistent flow into the canyon near the floor, and out of the canyon closer to the rim.

3.2 Spectral analysis

Power spectral density (PSD) plots were created from rotated, NaN interpolated, depth truncated, mean removed velocity data using a Welch method FFT, with parameters set according to the length of each data set, and a 15-minute resolution for ideal averaging of spectral features for interpretation. For clarity of interpretation, depth-specific results are plotted along with notable constituent frequencies, 95% confidence intervals, expected continuum slopes, and depth-average spectra. Specific depths were selected through a visual analysis of velocity plots to generally reduce the presence of NaN values and for optimal separation, typically between 50-100 metres from the minimum and maximum depth values obtained by each ADCP.

Rotary spectra were created from similar data as for PSD, and based on the work of Thomson (2014) and Gonella (1972) to determine the CW, CCW, and other necessary FFT components. Rotary analysis plots will be developed in both 1D and 2D formats, to better highlight rotational frequency trends through depth and time.

Spectrograms were generated using similar methods and parameters as the PSD spectra, and 'whitened' for visual clarity (multiplying spectrogram output by frequency squared). Specific depths were chosen for optimal upper and lower values, as in the PSD spectra, for comparison. Notable constituent frequencies are plotted for reference.

The classical GM spectrum for this region was generated from buoyancy data calculated using the Seawater package from regular seasonal CTD casts by DFO, at Line P Station P4 about 27 km from Barkley Canyon, though some adjustments are still necessary. For more details, see the Buoyancy and Density section, below.

Notable trends in PSD analysis include strong depth dependence for tidal constituents, and lesser seasonal dependence, with M_2 generally dominating

and f weakening at lower depths. There are potential sum peaks in the Upper Slope data for fM_2 and M_4, and three notable high frequency peaks consistent in the Axis data that have yet to be evaluated. There is also a flattening of the continuum at higher frequencies that could be associated with the instrument noise floor (to be determined).

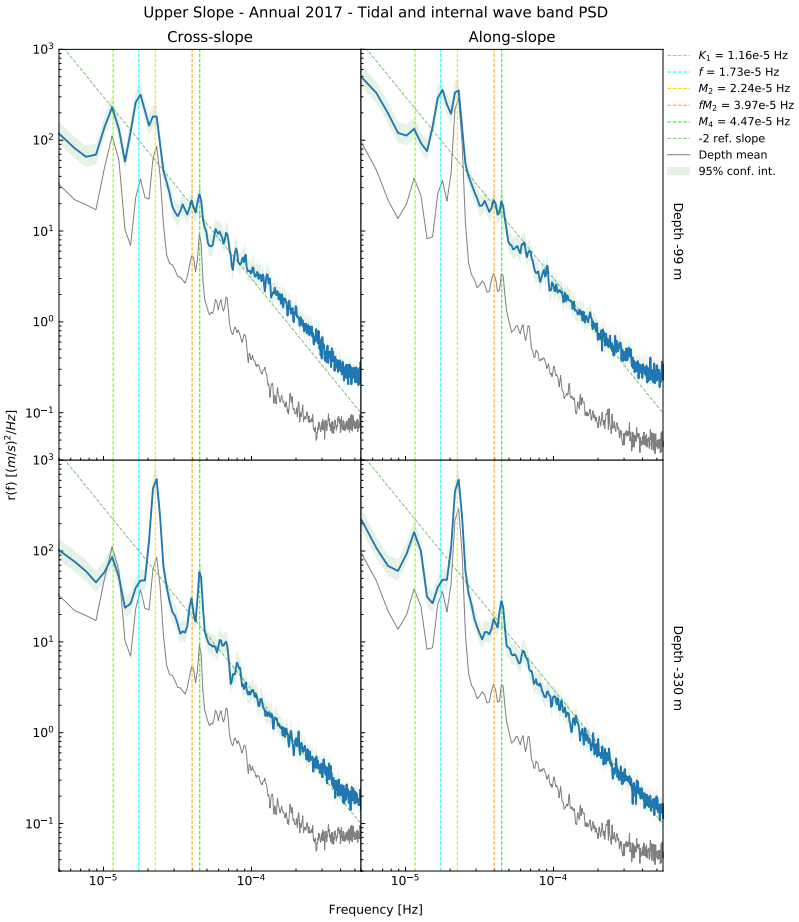

Figure 5: Annual PSD data for Upper Slope 75 kHz ADCP, in 2017. PSD show the cross- (left) and along-slope (right) velocity data, at an upper depth of -99 m (top) and lower depth of -330 m (bottom). PSD were processed using mean-removed and cleaned velocity data (see above), and optimised Welch FFT parameters.

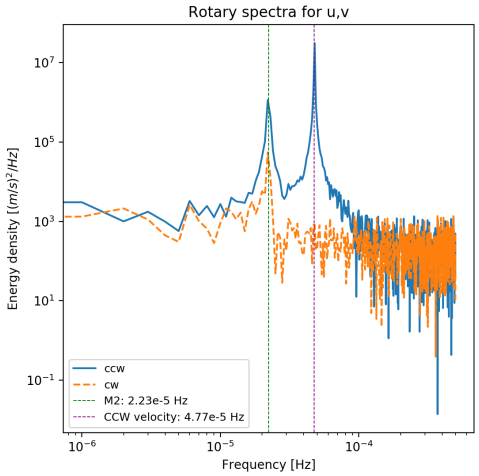

Figure 6: Test case output for rotary spectral analysis. Perfectly circular velocity data were simulated with generated noise, and a persistent M2 tidal constituent added in mostly u, to check the quality of the personally developed Python process, based on the work of Gonella and Thomson.

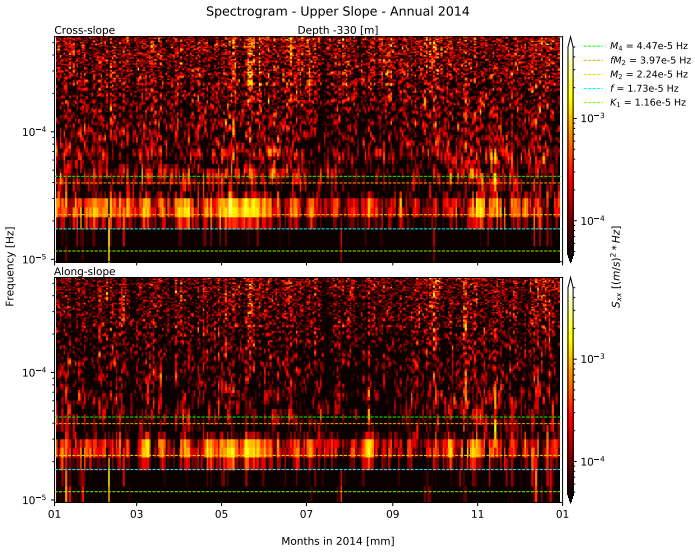

Figure 7: Whitened, comparative spectrogram data for Upper Slope 75 kHz ADCP, at -99 metres depth, 2014. Spectrograms are for the cross- (upper) and along-slope (lower) velocity data. Spectrograms were processed using mean-removed and cleaned velocity data (see above), optimised Welch FFT parameters, and whitened for visual clarity.

Notable spectrogram observations include a lack of high-frequency activity in the summer, possibly corresponding to a lack of storms. Though this seasonality is less prominent in the cross-slope direction, this direction also features more consistent high-frequency activity. Lower depths appear to show less seasonality, corresponding to PSD findings.

3.3 Buoyancy and density

Climatology data from annual Line P cruises allow for buoyancy and density calculations through depth, which can provide insight into changes to the fine-scale structure of the water column. Notable changes to stratification can be compared with the results of ADCP data analysis to reinforce assumptions regarding local internal wave events.

CTD data from La Perouse/Line P cruises were formatted and imported to calculate in situ density, and find buoyancy frequency through depth. Barkley Canyon is centred at approximately 48.33°N 126.03°W, so Rosette (deep) CTD casts from Station P4 are closest (approximately Lat 48.39 Long -126.39); a distance of about 27 km. Winter CTD casts were within January/February, and summer casts were within August/September. The Seawater Python package for determining ocean characteristics was used to calculate density, $\rho(z)$, and the Brünt-Väisälä Frequency squared (N^2(z)), based on the UNESCO 1983 (EOS 80) polynomial, at the mid-depths from the equation:

$$N^2 = \frac{-g}{\sigma_\theta}\frac{d\sigma_\theta}{dz}$$

where σ_θ is the density based on potential temperature values. These were then applied to a modified Python GM toolbox to generate a GM spectrum based on the local climatology and characteristics.

There is some seasonality in buoyancy data, though there is far more variability in depths above -200 metres, particularly in the summer. These depths are mostly irrelevant for a comparison with ADCP data between approximately -900 m and -100 m, and buoyancy frequency (N^2) is fairly static below -200 m at approximately 1×10^{-5} $(rad/s)^2$.

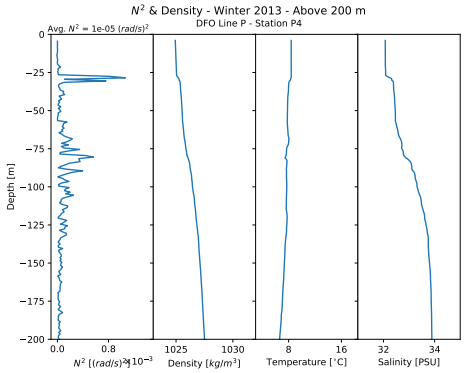

(a) Upper Winter

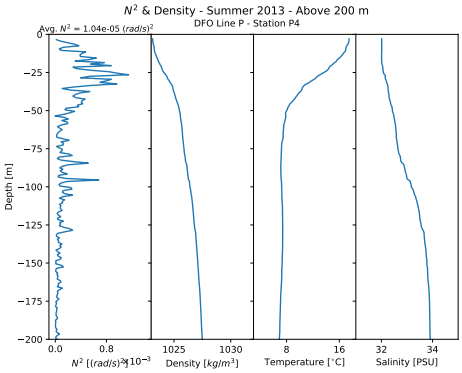

(b) Upper Summer

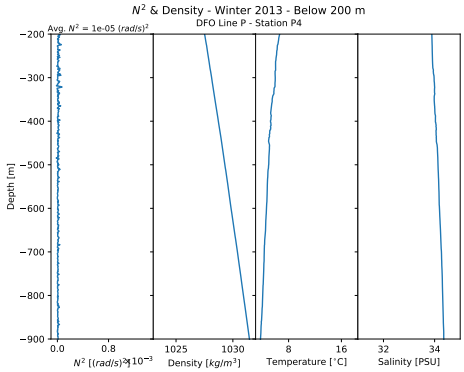

(c) Lower Winter

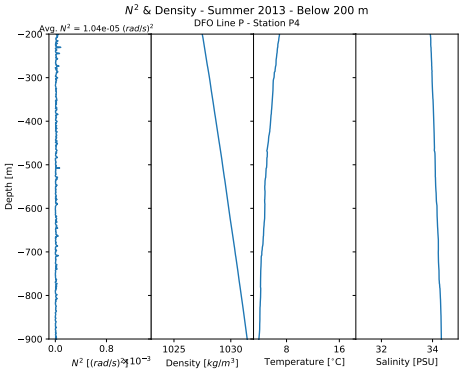

(d) Lower Summer

Figure 8: Seasonal N^2 and CTD data for Station P4 of Line P, collected by the DFO in 2013. The top row are upper depth plots (above -200 m), and the bottom row lower depth plots (below -200 m). Each plot shows N^2, density, temperature, and salinity, in order.

4 Relevant reading

Alford, M. H., Mackinnon, J. A., Zhao, Z., Pinkel, R., Klymak, J., Peacock, T., ... Peacock, T. (2007). Internal waves across the Pacific. Geophys. Res. Lett, 34, 24601. https://doi.org/10.1029/2007GL031566

Alford, M. H., Cronin, M. F., & Klymak, J. M. (2012). Annual cycle and depth penetration of wind-generated near-inertial internal waves at ocean station papa in the northeast pacific. Journal of Physical Oceanography, 42(6), 889–909. https://doi.org/10.1175/JPO-D-11-092.1

Allen, S. E., Vindeirinho, C., Thomson, R. E., Foreman, M. G. G., & Mackas, D. L. (2001). Physical and biological processes over a submarine canyon during an upwelling event. Canadian Journal of Fisheries and Aquatic Sciences, 58(4), 671–684. https://doi.org/10.1139/f01-008

Carter, G. S., & Gregg, M. C. (2002). Intense, Variable Mixing near the Head of Monterey Submarine Canyon. In Journal of Physical Oceanography (Vol. 32). https://doi.org/10.1175/1520-0485(2002)032¡3145:IVMNTH¿2.0.CO;2

Garrett, C., & Munk, W. (1979). Internal Waves in the Ocean. Ann. Rev. Fluid Mech., 11, 339–369.

Gemmrich, J., & Klymak, J. M. (2015). Dissipation of internal wave energy generated on a critical slope. Journal of Physical Oceanography, 45(9), 2221–2238. https://doi.org/10.1175/JPO-D-14-0236.1

Gilmour, A. (1987). A preliminary rotary spectral analysis of inertial currents off the west coast of New Zealand. New Zealand Journal of Marine and Freshwater Research, 21, 353–357. 10.1080/00288330.1987.9516231

Gonella, J. (1972). A rotary-component method for analysing meteorological and oceanographic vector time series (Vol. 19). Pergamon Press.

Hendershott, M., & Garrett, C. (2018). Lecture 6: Internal tides. Geophysical Fluid Dynamics, Woods Hole Oceanographic Institute. Retrieved from https://gfd.whoi.edu/wp-content/uploads/sites/18/2018/03/lecture0621356.pdf

Kelly, S., Nash, J., & E.Kunze. (2010). Internal-tide energy over topography. J. Geophys. Res., 115, C06014. doi.org/doi:10.1029/2009JC005618

Klymak, J. M., Alford, M. H., Pinkel, R., Lien, R. C., Yang, Y. J., & Tang, T. Y. (2011). The breaking and scattering of the internal tide on a

continental slope. Journal of Physical Oceanography, 41(5), 926–945. https://doi.org/10.1175/2010JPO4500.1

Kunze, E. (2017). Internal-wave-driven mixing: Global geography and budgets. Journal of Physical Oceanography, 47(6), 1325–1345. Retrieved from https://doi.org/10.1175/JPO-D-16-0141.1

Kunze, E., Mackay, C., Mcphee-Shaw, E. E., Morrice, K., Girton, J. B., & Terker, S. R. (2012). Turbulent mixing and exchange with interior waters on sloping boundaries. Journal of Physical Oceanography, 42(6), 910–927. https://doi.org/10.1175/JPO-D-11-075.1

MacKinnon, J., Zhao, Z., Whalen, C., Waterhouse, A., Trossman, D., Sun, O., ... Alford, M. (2017). Climate process team on internal wave-driven ocean mixing. Bulletin of the American Meteorological Society, 98(11), 2429–2454. doi.org/10.1175/BAMS-D-16-0030.1

Martini, K. I., Alford, M. H., Kunze, E., Kelly, S. M., & Nash, J. D. (2013). Internal bores and breaking internal tides on the Oregon continental slope. In Journal of Physical Oceanography (Vol. 43). https://doi.org/10.1175/JPO-D-12-030.1

Mihaly, S., Thomson, R., & Rabinovich, A. (1998). Evidence for nonlinear interaction between internal waves of inertial and semidiurnal frequency. Geophysical Research Letters, 25(8), 1205–1208. Retrieved from https://doi.org/10.1029/98GL00722

Munk, W., & Garret, C. (1979). 9: Internal Waves and Small-Scale Processes.

Nash, J., Kunze, E., Toole, J., & Schmitt, R. (2004). Internal Tide Reflection and Turbulent Mixing on the Continental Slope. American Meteorological Society. Retrieved from http://journals.ametsoc.org/jpo/article-pdf/34/5/1117/4470231/1520-0485

Ocean Networks Canada. (2013). Barkley Canyon. Retrieved from https://www.oceannetworks.ca/introduction-barkley-canyon

Ocean Networks Canada. (2020). Oceans 2.0. Retrieved from https://data.oceannetworks.ca/DataSearch

Rainville, L., & Pinkel, R. (2006). Propagation of Low-Mode Internal Waves through the Ocean. Retrieved from http://journals.ametsoc.org/jpo/article-pdf/36/6/1220/4483319/jpo28891.pdf

Robertson, R., Dong, J., & Hartlipp, P. (2017). Diurnal Critical Latitude and the Latitude Dependence of Internal Tides, Internal Waves, and Mixing

Based on Barcoo Seamount. Journal of Geophysical Research: Oceans, 122(10), 7838–7866. https://doi.org/10.1002/2016JC012591

Terker, S. R., Girton, J. B., Kunze, E., Klymak, J. M., & Pinkel, R. (2014). Observations of the internal tide on the California continental margin near Monterey Bay. Continental Shelf Research, 82, 60–71. https://doi.org/10.1016/j.csr.2014.01.017

Thomson, R. E., & Emery, W. J. (2014). Data analysis methods in physical oceanography (Third ed.). Oxford, UK; Elsevier.

Thomson, R. E., & Krassovski, M. V. (2015). Remote alongshore winds drive variability of the California Undercurrent off the British Columbia-Washington coast. Journal of Geophysical Research: Oceans, 120(12), 8151–8176. https://doi.org/10.1002/2015JC011306